Eur J Nucl Med Mol Imaging (2008) 35:2245–2255
DOI 10.1007/s00259-008-0845-7

ORIGINAL ARTICLE

Development and preclinical characterisation of ^{99m}Tc-labelled Affibody molecules with reduced renal uptake

Torun Ekblad · Thuy Tran · Anna Orlova · Charles Widström · Joachim Feldwisch · Lars Abrahmsén · Anders Wennborg · Amelie Eriksson Karlström · Vladimir Tolmachev

Received: 6 February 2008 / Accepted: 11 May 2008 / Published online: 2 July 2008

Abstract
Purpose Affibody molecules are low molecular weight proteins (7 kDa), which can be selected to bind to tumour-associated target proteins with subnanomolar affinity. Because of rapid tumour localisation and clearance from nonspecific compartments, Affibody molecules are promising tracers for molecular imaging. Earlier, ^{99m}Tc-labelled Affibody molecules demonstrated specific targeting of tumour xenografts. However, the biodistribution was suboptimal either because of hepatobiliary excretion or high renal uptake of the radioactivity. The goal of this study was to optimise the biodistribution of Affibody molecules by chelator engineering.
Materials and methods Anti-HER2 $Z_{HER2:342}$ Affibody molecules, carrying the mercaptoacetyl-glutamyl-seryl-glutamyl (maESE), mercaptoacetyl-glutamyl-glutamyl-seryl (maEES) and mercaptoacetyl-seryl-glutamyl-glutamyl (maSEE) chelators, were prepared by peptide synthesis and labelled with ^{99m}Tc. The tumour-targeting capacity of these conjugates was compared with each other and with the best previously available conjugate, ^{99m}Tc-maEEE-$Z_{HER2:342}$, in nude mice bearing SKOV-3 xenografts. The tumour-targeting capacity of the most promising conjugate, ^{99m}Tc-maESE-$Z_{HER2:342}$, was compared with radioiodinated $Z_{HER2:342}$.
Results All novel conjugates demonstrated successful tumour targeting and a low degree of hepatobiliary excretion. The renal uptakes of serine-containing conjugates, 33±5, 68±21 and 71±10%IA/g, for ^{99m}Tc-maESE-$Z_{HER2:342}$, ^{99m}Tc-maEES-$Z_{HER2:342}$ and ^{99m}Tc-maSEE-$Z_{HER2:342}$, respectively, were significantly reduced in comparison with ^{99m}Tc-maEEE-$Z_{HER2:342}$ (102±13%IA/g). For ^{99m}Tc-maESE-$Z_{HER2:342}$, a tumour uptake of 9.6±1.8%IA/g and a tumour-to-blood ratio of 58±6 were reached at 4 h p.i.
Conclusions A combination of serine and glutamic acid residues in the chelator sequence confers increased renal excretion and relatively low renal uptake of ^{99m}Tc-labelled Affibody molecules. In combination with preserved targeting capacity, this improved imaging of targets in abdominal area.

T. Ekblad · A. E. Karlström
School of Biotechnology, Royal Institute of Technology,
Stockholm, Sweden

T. Tran · A. Orlova · J. Feldwisch · V. Tolmachev
Unit of Biomedical Radiation Sciences, Rudbeck Laboratory,
Uppsala University,
Uppsala, Sweden

A. Orlova · J. Feldwisch · L. Abrahmsén · A. Wennborg · V. Tolmachev
Affibody AB,
Bromma, Sweden

C. Widström
Section of Hospital Physics, Department of Oncology,
Uppsala University Hospital,
Uppsala, Sweden

V. Tolmachev
Unit of Nuclear Medicine, Department of Medical Sciences,
Uppsala University,
Uppsala, Sweden

V. Tolmachev (✉)
Biomedical Radiation Sciences, Rudbeck Laboratory,
Uppsala University,
Uppsala, Sweden
e-mail: Vladimir.Tolmachev@bms.uu.se

Keywords Affibody molecule · HER2 · Renal uptake · Technetium-99m · Tumour targeting

Introduction

The attention of current nuclear medicine is shifting from the imaging of physiology and metabolism to the imaging of molecular structures, which are aberrantly presented on the surface of cancer cells or in the extracellular matrix [1]. This may provide information to guide the choice of the best treatment for a particular patient. Monoclonal antibodies have often been used for targeting, but their large size (approximately 150 kDa) causes slow blood clearance, slow extravasation and slow tumour penetration. Good imaging contrast, i.e., a high ratio of radioactivity concentrations between tumour and normal tissues, can therefore be obtained only several days after injection [2]. Data on tumour targeting using radiolabelled peptides and antibody fragments suggest that reduction of tracer size may increase imaging contrast because of more rapid tumour localisation and faster clearance from blood and healthy tissues [3, 4]. For the moment, the smallest immunoglobulin-based targeting agents used are the scFv, with a molecular weight of ~27 kDa [5] and single domain camelid antibody fragments with a molecular weight of 15 kDa [6].

The use of alternative non-immunoglobulin scaffolds makes it possible to create protein-based tracers with a smaller size than the antibody fragments [7]. One successful example is Affibody molecules; small (7 kDa) robust proteins, which can be selected to bind molecular targets with very high affinity [8, 9]. The Affibody molecule $Z_{HER2:342}$ binds the HER2 receptor with an affinity of 22 pM [10]. Overexpression of HER2 is detected in 25–30% of breast cancer patients, and treatment with the anti-HER2 antibody trastuzumab prolongs survival in these patients [11]. Current methods for assessment of HER2 expression are based on analysis of samples from the resected primary tumour or on biopsies, which may yield false-negative results because of expression heterogeneity and discordance in expression between primary tumours and metastases [12]. In contrast, radionuclide imaging could potentially provide a global picture of HER2 expression in all the patient's lesions.

Affibody molecules labelled with ^{111}In and ^{125}I have previously demonstrated high-contrast imaging of expression of HER2 in tumour xenografts within a few hours after injection [10, 13–16], and successful clinical imaging of HER2-expressing metastases was demonstrated using ^{111}In and ^{68}Ga-labelled Affibody molecules [17, 18]. Recently, selection of Affibody molecules, binding to another important molecular target, EGFR, was reported [19, 20]. Thus, Affibody molecules might open up new prospects in molecular radionuclide imaging, provided that appropriate labelling techniques are developed.

Technetium-99m (^{99m}Tc; $T_{1/2}$= 6 h) is the most attractive radionuclide utilised for SPECT. The energy of its gamma-quanta (140.5 keV) is nearly optimal for this application, the dose burden to the patient is usually low and a generator production provides low price and facile logistics. Therefore, ^{99m}Tc-labelled Affibody molecules might be rapidly implemented into clinical practice, despite challenging chemistry. Earlier, we have reported that introduction of the mercaptoacetyl-glycyl-glycyl-glycyl (maGGG) chelator into the anti-HER2 Affibody molecule $Z_{HER2:342}$ enabled stable labelling with ^{99m}Tc [21]. However, imaging of abdominal lesions could not be performed until one day after injection because of a high level of hepatobiliary excretion. Further experiments demonstrated that introduction of the more hydrophilic amino acid serine instead of glycine into the chelator sequence resulted in a shift of the excretion pathway from hepatobiliary to renal and reduced the radioactivity of the intestine content in mice to one third [22]. Further reduction of the hepatobiliary excretion would be desirable and when the charged, hydrophilic amino acid glutamic acid was introduced (with the maEEE chelator), the total radioactivity in the gastrointestinal tract was reduced to 3% of the injected radioactivity, creating a potential for high-contrast imaging in the abdomen [23]. Concomitantly, the renal uptake increased from 33.6±1.7% IA/g for ^{99m}Tc-maSSS-$Z_{HER2:342}$ to 95±23% IA/g for ^{99m}Tc-maEEE-$Z_{HER2:342}$ at 4 h p.i.

In the present study, we wanted to evaluate if the combination of serine and glutamic acid in the chelator might reduce the renal uptake of ^{99m}Tc-labelled Affibody molecules without an undesirable increase of abdominal radioactivity. To test this hypothesis, we have prepared several variants of Affibody molecules containing serine and glutamic acid in the chelating sequence (Fig. 1), and performed a comparative biodistribution study of ^{99m}Tc-maEEE-$Z_{HER2:342}$, ^{99m}Tc-maESE-$Z_{HER2:342}$, ^{99m}Tc-maEES-$Z_{HER2:342}$, and ^{99m}Tc-maSEE-$Z_{HER2:342}$ in a murine xenograft model.

Materials and methods

Radioactivity measurements Radioactivity in cells and biological samples was measured using an automated gamma-counter with a 3-in. NaI(Tl) detector (1480 WIZARD, Wallac Oy, Turku, Finland). Radioactivity distribution along instant thin layer chromatography (ITLC) strips and on sodium dodecyl sulfate polyacrylamide gel electrophoresis (SDS-PAGE) gels was detected on the Cyclone™ Storage Phosphor System and the OptiQuant™ image analysis software (Perkin Elmer, Wellesley, MA, USA). A

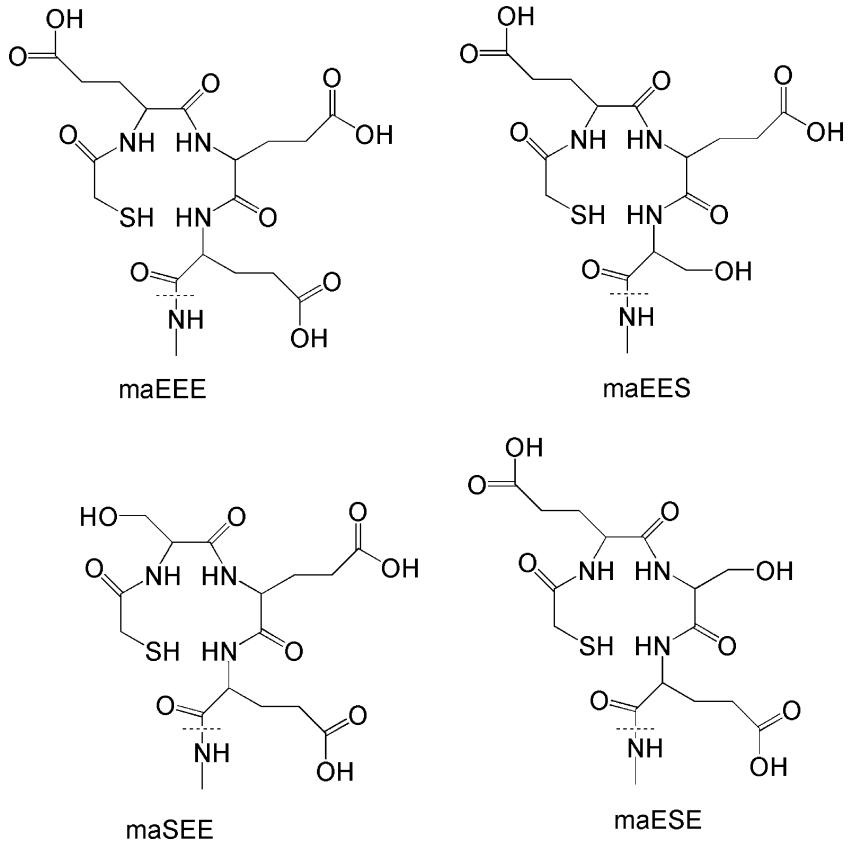

Fig. 1 Structures of the maEEE, maEES, maSEE and maESE chelators

dual-head e.Cam gamma camera (Siemens Medical Systems), equipped with a low-energy, high-resolution (LEHR) collimator was used for imaging. Acquisition of static images was performed with a 256×256 matrix and a zoom factor of 3.2. The energy window settings were 140 keV, 15%.

Peptide synthesis and characterisation of Affibody molecules Automated Fmoc/tBu solid phase peptide synthesis was performed on a 433APeptide Synthesizer (Applied Biosystems, Foster City, CA, USA) as described in [24] using 10 molar equivalents of HBTU, HOBt and Fmoc-protected amino acid for each coupling and a Fmoc-amide resin with a substitution of 0.67 mmol/g (Applied Biosystems). All reagents were of synthetic grade as described in [22]. Incompletely acylated peptides were terminated with acetic anhydride.

The Tc-chelating moieties were added sequentially by manual synthesis as N-terminal extensions of the $Z_{HER2:342}$ peptide. Peptides were released from solid support and deprotected by a 2 h incubation in TFA:EDT:H_2O:TIS (94:2.5:2.5:1) followed by extraction with *tert*-butyl methyl ether: H_2O (50:50) three times before filtration and lyophilisation.

Analytical and preparative RP-HPLC were run using a 4.5×150 mm polystyrene/divinylbenzene matrix column with a particle size of 5 μm (Amersham Biosciences) at a flow rate of 1 ml/min and a 20 min elution gradient of 20–60% B or 20–40% B (A: 0.1% TFA–H_2O, B: 0.1% TFA–CH_3CN). Full-length products were identified by mass spectrometric analyses on a Q-Tof™ II mass spectrometer with an ESI source (Waters Corporation, Micromass MS Technologies, Manchester, UK). The concentration of each peptide was determined by amino acid analysis, performed by Aminosyraanalyscentralen, (Uppsala, Sweden).

The melting point of each protein was established by variable temperature measurements from 20 °C to 90 °C at 221 nm as in [22]. A circular dichroism wavelength scan from 250 nm to 195 nm was collected before and after melting.

Recombinant Human ErbB2/Fc Chimera from R&D Systems was used as immobilized ligand in real-time biospecific interaction analyses, performed on a Biacore 2000 (Biacore, Sweden). Human serum albumin, (HSA; KabiVitrum, Sweden) was immobilised as a reference on one surface of the CM5 sensor chip (Biacore AB, Sweden). Affibody molecules diluted in HBS (10 mM Hepes, 150 mM NaCl, 3.4 mM ethylenediaminetetraacetic acid (EDTA), 0.005% Surfactant P20, pH 7.4) running buffer were used as analytes. The binding kinetics were studied using analyte concentrations in the range of 0.5–20 nM, a 5

min association phase and a 10 min dissociation phase (as described in [22]). Kinetic constants were calculated by using the Langmuir 1:1 binding model in the BiaEval software (Biacore AB, Sweden).

Labelling with ^{99m}Tc and in vitro stability testing ^{99m}Tc was obtained as pertechnetate from an Ultra-TechneKow generator (Tyco) by elution with sterile 0.9% NaCl (Mallinckrodt Medical BV, Petten, Holland). Yield, radiocolloid content and radiochemical purity of the labelled Affibody constructs were analysed by instant thin layer chromatography on silica gel impregnated glass fiber sheets, ITLC strips (ITLC™ SG, from Gelman Sciences) as described in [22].

Labelling was performed according to [22]. In brief, the pH of the Affibody samples was adjusted to 11 by addition of NaOH. A solution of $SnCl_2$*$2H_2O$ in 0.01 M HCl (10 µl, 1 mg/ml) was added followed by addition of the fresh pertechnetate solution. The labelling mixture was incubated for 1 h at room temperature, purified on NAP-5 columns (Amersham Pharmacia Biotech AB, Sweden) and analysed by ITLC.

The stability of the labelled Affibody conjugates was tested in excess of cysteine and in murine serum. All experiments were performed in triplicate as described in [21]. Briefly, 300-fold molar excess of cysteine was mixed with the radiolabelled Affibody ligand, incubated for 2 h at 37 °C and analysed by ITLC. The labelled Affibody conjugate was diluted in serum from The Naval Medical Research Institute (NMRI) mice to a concentration resembling the blood level at the moment of injection and incubated at 37 °C for 2 h. The mixture was analysed on NuPAGE 4–12% Bis–Tris Gel (Invitrogen) in MES buffer (200 V constant), using pertechnetate as a size reference to study the radioactivity distribution along the gel.

Cell binding and retention studies SKOV-3 cells with approximately 1.2×10^6 HER2 receptors per cell (purchased from ATCC via LGC Promochem AB, Boras, Sweden), were cultured in McCoy's medium (Flow Irvine, UK) supplemented with 10% fetal calf serum (Sigma, USA), 2 mM L-glutamine, and PEST (penicillin 100 IU/ml and 100 µg/ml streptomycin; all from Biokrom Kg, Germany) at 37 °C in a humidified incubator with 5% CO_2 and trypsinised using a trypsin–EDTA solution (0.25% trypsin, 0.02% EDTA; Biokrom Kg, Germany) as described in [22]. Cells were counted in an electronic cell counter (Beckman Coulter, Fullerton, CA, USA).

The binding specificity was tested on HER2-expressing cells as described in [22]. Essentially, the labelled conjugates were added to two sets of Petri dishes with a calculated ratio of one labelled conjugate per HER2 receptor. One group of dishes was pre-saturated with a 100-fold excess of non-labelled Affibody molecule 10 min before the labelled conjugate was added. The cells were incubated for 1 h at 37 °C and the radioactivity in the incubation medium, and the resuspended cells were counted.

The cellular retention was determined as in [21]. Briefly, the labelled conjugate was incubated with SKOV-3 cells at 37 °C for 2 h. The association was interrupted by washing with ice-cold serum-free medium, and the cell-bound radioactivity was measured in an automated gamma-counter after 0.5, 1, 2, 4, 8 or 24 h of further incubation.

In vivo experiments All animal studies were performed in accordance with Swedish law and were approved by the Uppsala Committee of Animal Research Ethics. The tumour xenograft model was obtained by subcutaneously (s.c.) injecting ~5*10^6 SKOV-3 cells in the hind leg of female outbreed BALB/c *nu/nu* mice 4–6 weeks before the experiment as described in [22].

The biodistribution study was performed as in [22]. The mice were anesthetised by an intraperitoneal injection of ketamine HCl (Ketalar, Pfizer) and xylazine HCl (Rompun; Bayer) at predetermined time points after injection of the radiolabelled conjugate. Thereafter, the mice were euthanised through heart puncture, and blood and organ samples were collected. Organ uptake values were calculated as percent injected activity per gram tissue (% IA/g) except for the thyroid and intestines, which were measured as whole organs. In all experiments, the mice were randomly divided into groups of four animals.

The biodistribution pattern of ^{99m}Tc-maEEE-$Z_{HER2:342}$, ^{99m}Tc-maESE-$Z_{HER2:342}$, ^{99m}Tc-maEES-$Z_{HER2:342}$ and ^{99m}Tc-maSEE-$Z_{HER2:342}$ were compared at 4 h p.i. Each group of mice was injected subcutaneously with 1 µg [~50 kBq in 100 µl phosphate-buffered saline (PBS)] of one of the conjugates. At 4 h p.i., the mice were euthanized, and organ samples of blood, lung, liver, spleen, kidney, tumour, stomach, muscle, thyroid and intestines were collected. In previous studies, we have validated that the biodistribution of radiolabelled Affibody molecules at 4 h p.i. is the same for both i.v. and s.c. injection and independent on the label [15, 25]. Biodistribution of Affibody molecules in mice after subcutaneous injections is usually more reproducible (smaller errors), which is important for comparative studies. This study was repeated twice, with different batches of radiolabelled conjugates, and the results have been pooled.

A study was performed to elucidate if the observed large difference in the renal accumulation of radioactivity between the different conjugates was caused by a difference in renal reabsorption or by a difference in retention of radiocatabolites in kidneys. ^{99m}Tc-maEEE-$Z_{HER2:342}$, ^{99m}Tc-maESE-$Z_{HER2:342}$, ^{99m}Tc-maEES-$Z_{HER2:342}$ and

^{99m}Tc-maSEE-$Z_{HER2:342}$ was i.v. injected in normal NMRI mice (two animals per conjugate). The animals were euthanized 15min after injection, and urine was collected. The urine was analysed by SDS-PAGE, as described for the serum stability test.

The conjugate with the lowest renal uptake, ^{99m}Tc-maESE-$Z_{HER2:342}$, was used in a follow-up biodistribution study with the aim to define the optimal imaging time point and also to directly compare the biodistribution of ^{99m}Tc-maESE-$Z_{HER2:342}$ with radioiodinated recombinant $Z_{HER2:342}$ and to confirm the specificity of tumour accumulation of ^{99m}Tc-maESE-$Z_{HER2:342}$. The recombinant Affibody molecule $Z_{HER2:342}$ was labelled with *N*-succinimidyl para-iodobenzoate (^{125}I-PIB-$Z_{HER2:342}$), as described by Orlova and coworkers [10]. Four groups of mice, with four animals per group, were injected subcutaneously with a mixture of ^{99m}Tc-maESE-$Z_{HER2:342}$ and ^{125}I-PIB-$Z_{HER2:342}$ (total protein dose 1 μg, ~100 kBq in 100 μl PBS). One group was used as a specificity control and was subcutaneously injected with 750 μg of cold recombinant $Z_{HER2:342}$ 40 min before injection of radiolabelled Affibody molecules to saturate the HER2 receptors in the tumours. The mice were euthanized at 1, 4 and 6 h p.i., as described above, and organ samples of blood, lung, liver, kidney, stomach, spleen, muscle, thyroid, bone, and tumour were collected for measurement of the radioactivity. The gastrointestinal tract was collected together with its content. In the specificity control group, blood and tumours were taken for the measurement. Gamma-spectrometry was used to discriminate between ^{125}I and ^{99m}Tc radioactivity.

Gamma-camera imaging Gamma-camera imaging studies were performed on mice bearing HER2-expressing xenografts, after intravenous injection into the tail vein of 10 MBq (3 μg) ^{99m}Tc-maESE-$Z_{HER2:342}$. At predetermined time points, a lethal dose of Rompun/Ketalar was injected, and the mice were sacrificed by cervical dislocation, before excision of the urinary bladders. Imaging was performed immediately using a Siemens e.Cam gamma-camera equipped with LEHR collimator at the Department of Nuclear Medicine of Uppsala University Hospital as described in [21].

To determine a suitable time for HER2-imaging, four mice with SKOV-3 xenografts were imaged simultaneously, two at 1 h p.i. and two at 2 h p.i. In addition, one mouse with BT 474 xenograft sacrificed at 2 h p.i. was imaged. In the second study, the specificity of HER2-targeting was confirmed. Two mice were injected with ^{99m}Tc-maESE-$Z_{HER2:342}$, and one animal was pre-injected with 1 mg of non-labelled $Z_{HER2:342}$ to saturate the HER2-recptors in tumours. Both mice were imaged simultaneously 5 h after the injection of ^{99m}Tc-maESE-$Z_{HER2:342}$.

Results

Peptide synthesis and characterisation of Affibody molecules The data concerning preparation and characterization of the Affibody molecules are presented in Table 1. The full-length Affibody molecule $Z_{HER2:342}$ was obtained at a 21% yield, and the manual introduction of the chelators reduced the total synthetic yield to 12–14%. The molecular weights of the different conjugates were in good agreement with the theoretically calculated masses. The melting points varied between 62 °C and 68 °C.

The circular dichroism spectra indicated that the Affibody molecules refolded after heating to 90 °C without loss of helicity. All conjugates displayed a strong binding affinity to HER2, with dissociation constants varying within 230–500 pM.

Labelling with ^{99m}Tc and in vitro stability testing The ^{99m}Tc labelling yield was approximately 90%, and all labelled conjugates could be obtained at a purity higher than 95%, as summarised in Table 1. A thiol challenge was performed to study the stability of the ^{99m}Tc attachment to Affibody molecules, demonstrating that 80–90% of the technetium was still attached to the Affibody molecules after 2 h incubation in 300-fold molar excess of cysteine.

The results of the serum stability tests are presented in Fig. 2. The single radioactivity peak corresponds to the position of the Affibody molecule. No radioactivity was

Table 1 Affibody molecules used in this study

Peptide	Synthesis yield (%)	Calculated/experimental Mw (Da)	T_m (°C)	K_D (pM)	Labelling yield (%)	Isolated labelling yield (%)	Radio-chemical purity (%)
maSEE-$Z_{HER2:342}$	14	7,138/7,138	65	490	92±0.4	74±2	97±1
maESE-$Z_{HER2:342}$	12	7,138/7,138	62	500	87±8	75±1	97±2
maEES-$Z_{HER2:342}$	12	7,138/7,138	63	230	90±6	74±1	99±1
maEEE-$Z_{HER2:342}$	13	7,180/7,179	68	410	90±2	76±4	98±2

Data on labelling yield, isolated yield and purity are presented as an average from at least ten labelling experiments. Colloid content was always less than 2%.

maEEE-$Z_{HER2:342}$ has been used for comparison. Data on molecular weight, melting point and affinity are taken from [23].

found to be trans-chelated to blood plasma proteins. A very small amount of radioactivity was associated with low-molecular weight species, indicating that the chelate is highly stable and, also, that the Affibody molecules are not degraded during circulation.

Cell binding and retention studies The binding of ^{99m}Tc-maEES-$Z_{HER2:342}$, ^{99m}Tc-maSEE-$Z_{HER2:342}$ and ^{99m}Tc-maESE-$Z_{HER2:342}$ conjugates to HER2-expressing SKOV-3 cells could be blocked by the addition of a 100-fold excess of non-labelled $Z_{HER2:342}$ ($p < 0.0001$), proving the HER2-binding specificity for all conjugates. The cellular retention was high and quite similar for all the labelled conjugates during the first 8 h. The cell-associated radioactivity decreased to 82±2, 82±0.3 and 84±1% during the first hour for ^{99m}Tc-maEES-$Z_{HER2:342}$, ^{99m}Tc-maSEE-$Z_{HER2:342}$ and ^{99m}Tc-maESE-$Z_{HER2:342}$, respectively, and dropped to 81±3, 77±0.3 and 75±3% after 8 h. So, the difference was within the accuracy of the method. Twenty-four hours after media change, 61±4 and 58±3% of the radioactivity was cell-associated for ^{99m}Tc-maSEE-$Z_{HER2:342}$ and ^{99m}Tc-maESE-$Z_{HER2:342}$, respectively. The retention of ^{99m}Tc-maEES-$Z_{HER2:342}$ was somewhat better, with 74±1% radioactivity still associated with cells.

Biodistribution experiments Data on the comparative biodistribution of ^{99m}Tc-maEEE-$Z_{HER2:342}$, ^{99m}Tc-maESE-$Z_{HER2:342}$, ^{99m}Tc-maEES-$Z_{HER2:342}$ and ^{99m}Tc-maSEE-$Z_{HER2:342}$ at 4 h p.i. are presented in Table 2. The distribution pattern of ^{99m}Tc-maEEE-$Z_{HER2:342}$ was in good agreement with the results from a previous study [23]. The general pattern was very similar between all the conjugates, with a quick clearance from blood, nonspecific compartments and the carcass. The average radioactivity in the gastrointestinal tract was below 5% for all mercaptoacetyl-diglutamyl-seryl variants, showing that the desirable reduction of the hepatobiliary excretion was achieved. The uptake in the tumour was higher than in any organ and tissue, except for the kidneys. The tumour-to-blood radioactivity concentration ratio exceeded 20 for all conjugates, and should allow for a high-contrast imaging. There was, however, a pronounced difference in the kidney uptake. All mercaptoacetyl-diglutamyl-seryl variants demonstrated a significant ($p<0.005$) reduction of the renal uptake of radioactivity in comparison with ^{99m}Tc-maEEE-$Z_{HER2:342}$, down to a third with ^{99m}Tc-maESE-$Z_{HER2:342}$. Moreover, the renal uptake of ^{99m}Tc-maESE-$Z_{HER2:342}$ was significantly lower ($p<0.005$) than the uptake of either ^{99m}Tc-maEES$Z_{HER2:342}$ or ^{99m}Tc-maSEE-$Z_{HER2:342}$.

To elucidate if the observed large difference in the renal accumulation of radioactivity between the different conjugates was caused by differences in renal reabsorption or by differences in retention of radiocatabolites in kidneys, a urine analysis was performed. Urine was collected from NMRI mice 15 min after intravenous injection of ^{99m}Tc-labelled Affibody molecules and analysed by SDS-PAGE. The measured radioactivity was in a low-molecular weight form for all conjugates, and no radioactivity was found to be associated with intact conjugates. This indicates a nearly complete reabsorption of the conjugates in the proximal

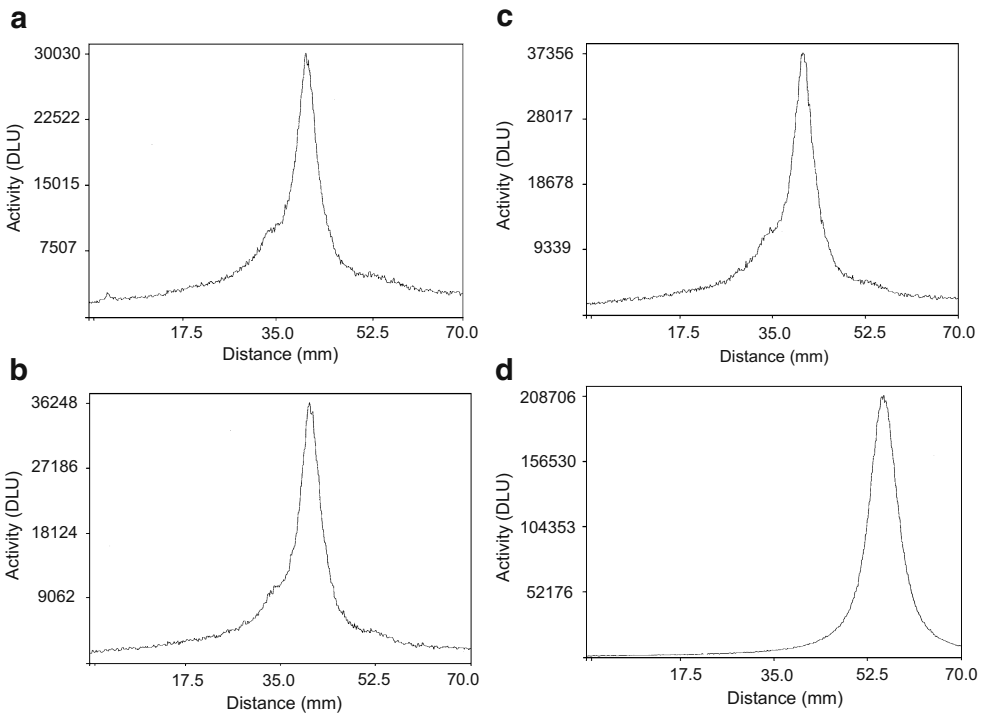

Fig. 2 Stability of radiolabeled conjugates in murine serum. The conjugates were incubated in murine serum at 37 °C for 2 h and analysed by SDS-PAGE. **a** ^{99m}Tc-maEES-$Z_{HER2:342}$, **b** ^{99m}Tc-maESE-$Z_{HER2:342}$, **c** ^{99m}Tc-maSEE-$Z_{HER2:342}$, **d** ^{99m}Tc-pertechnetate as a marker of low molecular weight catabolites

Table 2 Comparative biodistribution of ^{99m}Tc-maEEE-$Z_{HER2:342}$, ^{99m}Tc-maESE-$Z_{HER2:342}$, ^{99m}Tc-maEES-$Z_{HER2:342}$ and ^{99m}Tc-maSEE-$Z_{HER2:342}$ in BALB/c *nu/nu* mice bearing HER2-expressing SKOV-3 xenografts

Organ	^{99m}Tc-maEEE-$Z_{HER2:342}$	^{99m}Tc-maESE-$Z_{HER2:342}$	^{99m}Tc-maEES-$Z_{HER2:342}$	^{99m}Tc-maSEE-$Z_{HER2:342}$
Uptake, % IA/g				
Blood	0.27±0.08	0.17±0.03	0.24±0.11	0.16±0.03
Lung	0.33±0.11	0.21±0.05	0.35±0.30	0.21±0.09
Liver	0.57±0.13	0.33±0.06	0.90±0.31	0.48±0.07
Spleen	0.36±0.33	0.17±0.12	0.15±0.08	0.17±0.03
Stomach	1.34±0.30	0.56±0.15	0.72±0.53	0.53±0.10
Kidney	102±13	33±5[a,b]	68±21[a]	71±10[a]
Salivary gland	1.58±1.02	0.57±0.17	1.12±0.81	0.72±0.18
Thyroid	0.09±0.04	0.03±0.01	0.05±0.03	0.04±0.02
Tumour	8.08±1.36	9.65±1.82	12.22±4.03	10.28±2.01
Muscle	0.15±0.08	0.07±0.03	0.06±0.03	0.05±0.01
Intestine with content[c]	3.6±0.7	2.4±0.4	4.1±1.2	1.9±0.3
Carcass[c]	4.9±0.3	3.5±1.2	3.5±1.1	3.8±0.8
Tumour-to-organ ratio				
Blood	31±9	58±6	55±15	68±25
Liver	14±2	29±5	13±1	22±6
Kidney	0.079±0.012	0.297±0.045	0.181±0.036	0.145±0.027

Animals were s.c. injected, and data from two independent set of experiments, each with four animals per group, were combined. Uptake is expressed as % IA/g, and presented as an average value from eight animals±SD.
[a] Significant reduction of renal uptake in comparison with ^{99m}Tc-maEEE-$Z_{HER2:342}$
[b] Significant reduction of renal uptake in comparison with ^{99m}Tc-maEES-$Z_{HER2:342}$ and ^{99m}Tc-maSEE-$Z_{HER2:342}$
[c] Data for intestines with content and carcass are presented as % of injected radioactivity per whole sample

tubuli. The differences in renal accumulation among the Affibody variants might therefore be explained by differences in the retention of the corresponding radiocatabolites.

In the second study in tumour-bearing mice, the biodistribution of ^{99m}Tc-maESE-$Z_{HER2:342}$ was analysed at 1, 4 and 6 h p.i. (Table 3), confirming the low renal radioactivity uptake found in the previous experiment. In vivo blocking with non-labelled $Z_{HER2:342}$ demonstrated that the tumour uptake of ^{99m}Tc-maESE-$Z_{HER2:342}$ could be significantly ($p<0.0001$) reduced and, therefore, that the tumour targeting was HER2-specific. Tumour-to-organ ratios were similar at 4 and 6 h pi, suggesting that the optimal imaging time is between these time points. However, the tumour-to-blood ratio was more than five already at 1 h p.i., indicating that successful imaging is possible at this early time point. Direct comparison with the radioiodinated Affibody molecule showed that ^{99m}Tc-maESE-$Z_{HER2:342}$ provided a higher tumour uptake and a more rapid clearance from blood and non-tumour tissues.

Figure 3 shows a comparison of the biodistribution of ^{99m}Tc-maESE-$Z_{HER2:342}$ in nude mice 4 h after intravenous and subcutaneous injection. No significant difference could be detected.

Imaging experiments Gamma-camera images of mice bearing SKOV-3 xenografts are presented in Figs. 4 and 5. The images were acquired 1, 2 and 5 h after administration of ^{99m}Tc-maESE-$Z_{HER2:342}$. The tumours could be clearly visualised as early as 1 h p.i., and the image contrast improved over time. In addition to the decrease of whole-body radioactivity, the interference from kidney-associated radioactivity was lower at later time points. Tumour-to-non-tumour ratios for the contralateral thigh were 9±1, 26±4 and 40 at 1, 2 and 5 h p.i., respectively. In addition, visualisation of a xenograft that originates from the HER2-expressing cell line BT-474 was demonstrated 2 h p.i. In this case, the tumour-to-contralateral thigh ratio was 17. To prove that the tumour targeting by ^{99m}Tc-maESE-$Z_{HER2:342}$ was because of specific binding to HER2, one animal was pre-injected with an excess of non-labelled Affibody molecules. As shown in Fig. 5, this pretreatment reduced the accumulation of radioactivity in the tumour which is also reflected by a reduction of the tumour-to-contralateral thigh ratio from 40 to 3. No uptake in any other organs was seen, except in the kidneys, in concordance with biodistribution data.

Discussion

Manipulation of excretion pathways and uptake in excretory organs is an important issue in the design of targeting conjugates for molecular imaging. Affibody molecules constitute a platform for the development of radiolabelled conjugates for molecular imaging. One challenge is the shortage of knowledge concerning the factors that control

Table 3 Comparative biodistribution of ^{99m}Tc-maESE-$Z_{HER2:342}$ and ^{125}I-PIB-$Z_{HER2:342}$ after i.v. injection in BALB/c *nu/nu* mice bearing HER2-expressing SKOV-3 xenografts

Organ	1 h		4 h		6 h	
	^{99m}Tc-maESE-$Z_{HER2:342}$	^{125}I-PIB-$Z_{HER2:342}$	^{99m}Tc-maESE-$Z_{HER2:342}$	^{125}I-PIB-$Z_{HER2:342}$	^{99m}Tc-maESE-$Z_{HER2:342}$	^{125}I-PIB-$Z_{HER2:342}$
Uptake, % IA/g						
Blood	1.30±0.15	2.34±0.13	0.25±0.11 (0.31±0.03)[a]	0.51±0.04 (0.49±0.06)[a]	0.22±0.05	0.27±0.04
Lung	1.24±0.03	2.21±0.19	0.28±0.12	0.40±0.13	0.21±0.03	0.27±0.07
Liver	1.11±0.19	3.43±0.62	0.44±0.07	0.60±0.07	0.38±0.04	0.27±0.03
Spleen	0.36±0.20	0.89±0.49	0.19±0.08	0.18±0.04	0.14±0.05	0.11±0.02
Stomach	2.56±0.60	0.93±0.10	0.76±0.16	0.51±0.50	1.02±0.24	0.18±0.03
Kidney	117±16	29.90±5.50	35.03±1.58	12.82±2.51	27.12±2.48	7.64±1.16
Tumour	6.94±1.40	4.20±0.73	9.61±1.58 (0.44±0.09)[b]	4.22±1.41 (0.53±0.07)[b]	7.65±1.25	4.43±0.66
Muscle	0.20±0.11	0.29±0.17	0.09±0.04	0.07±0.01	0.07±0.03	0.06±0.04
Intestines with content[c]	3.50±0.42	4.44±0.52	2.99±0.74	3.08±0.47	2.89±0.62	0.91±0.40
Carcass[c]	11.6±1.1	31.01±1.10	7.55±3.28	8.96±0.99	5.06±0.89	7.03±0.90
Tumour-to-organ ratio						
Blood	5.5±1.5	1.8±0.4	45.9±19.8	8.2±2.4	37.1±11.1	16.5±3.5
Liver	6.3±1.1	1.2±0.1	21.9±3.0	7.0±1.9	20.3±3.8	16.5±3.6
Kidney	0.06±0.01	0.14±0.03	0.27±0.05	0.33±0.05	0.28±0.04	0.59±0.11

Uptake is expressed as % IA/g, and presented as an average value from four animals±SD.

[a] Data in parentheses represent values from animals pre-injected with excess of non-labelled $Z_{HER2:342}$. The difference in blood concentration of radioactivity between blocked and non-blocked animals was not significant.

[b] The difference in tumour uptake was significant ($p<0.005$).

[c] Data for intestines with content and carcass are presented as % of injected radioactivity per whole sample

the biodistribution of this novel class of targeting proteins. The intermediate size of the Affibody molecules does not allow direct translation of knowledge obtained for other classes of targeting agents. Affibody molecules are well

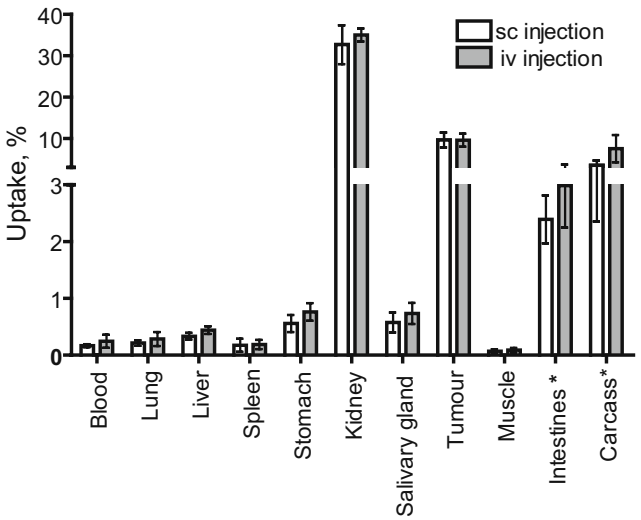

Fig. 3 Biodistribution of ^{99m}Tc-maESE-$Z_{HER2:342}$ 4 h after intravenous (i.v.) and subcutaneous (s.c.) injections in BALB/c *nu/nu* mice bearing HER2-expressing SKOV-3 xenografts. Uptake is expressed as % IA/g and presented as an average value from eight (s.c. injection) or four (i.v. injection) animals±SD. *Data for intestines with content and carcass are presented as % of injected radioactivity per whole sample

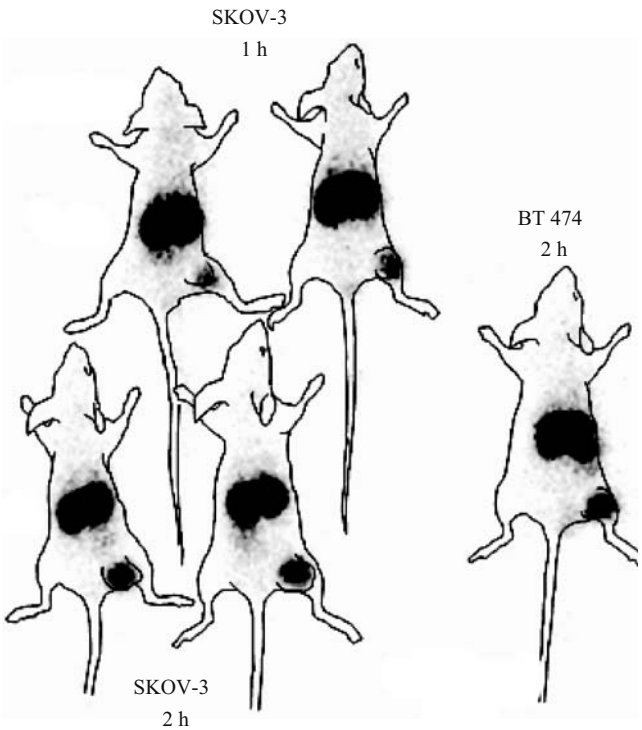

Fig. 4 Gamma-camera imaging of HER2-expressing xenografts in mice using ^{99m}Tc-maESE-$Z_{HER2:342}$. Contours derived from digital photographs are superimposed over gamma-camera images to facilitate interpretation

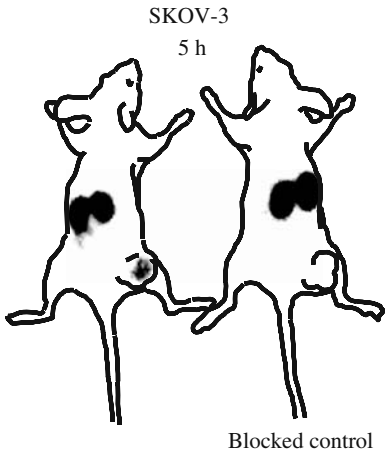

Fig. 5 Gamma-camera imaging of HER2-expressing xenografts in mice using ^{99m}Tc-maESE-$Z_{HER2:342}$. The right animal was pre-injected with unlabelled $Z_{HER2:342}$. Contours derived from digital photographs are superimposed over gamma-camera images to facilitate interpretation

below the cut-off for renal clearance, in contrast to several types of antibody fragments, yet in contrast to small peptides large enough for the chelating portion to be regarded as a separate entity in terms of effects on distribution properties. Thus, more work is required to find structure–property relationships for Affibody molecules, including different aspects of excretion pathway modification.

The hepatobiliary excretion creates problems when imaging targets in the abdomen because of an elevated background. Moreover, it can lead to false-positive findings because of occasional formation of hot spots. Our previous studies [21–23] were dedicated to the reduction of hepatobiliary excretion of ^{99m}Tc-labelled Affibody molecules. The molecules contained an N-terminal chelating sequence of mercaptoacetyl followed by three amino acid residues that were varied. These studies demonstrated that the substitution of a single amino acid in the chelating three amino acid sequence could alter both the biodistribution and the renal uptake appreciably. These efforts were successful in significantly reducing the hepatobiliary excretion, but at the cost of a significant increase in renal accumulation.

Renal excretion is preferred over hepatobiliary excretion, also when resulting in a high accumulation of radioactivity in the kidneys. The well-defined shape of the kidneys in combination with SPECT/CT reduces the risk of image misinterpretation. But high renal uptake might complicate imaging of lesions, which are located in close proximity to the kidneys. For this reason, a reduction of the renal retention of the radioactivity is desirable. Renal uptake is typical for all proteins and peptides, which have a size below the cut-off for glomerular filtration, approximately 60 kDa [26]. After passing glomeruli, short proteins and peptides are reabsorbed in the proximal tubuli of the kidney and degraded. It has recently been demonstrated that the scavenger receptor megalin is involved in reabsorption of somatostatin analogues from primary urine [27, 28]. It has been shown that the renal reabsorption of radiolabelled peptides might be suppressed by co-infusion of a number of substances, such as basic amino acids [29], polyglutamic acid [30] or gelofusine [31]. However, the selectivity of suppression (either by cationic amino acid or by polyglutamic acid) for different proteins indicates that there are several different scavenger receptors, which are involved in kidney uptake of radiolabelled proteins and peptides [32]. The use of cationic amino acids for co-infusion provided excellent results in radionuclide therapy using radiolabelled somatostatin analogues (see, e.g., [29] and [33]). However, the use of cationic amino acids in imaging is questionable because of side effects, such as nausea and vomiting. Besides patient discomfort, these side effects might decrease the sensitivity of imaging because of movement-associated artefacts. For this reason, a reduction of renal uptake by molecular design of the conjugate seems to be a better alternative.

The reduced hepatobiliary excretion found in the previous studies may result from either reduced hepatic uptake or that the metabolites are not ending up in the bile, or a combination of both. In the same way, renal accumulation may be reduced by reducing uptake in the proximal tubuli or from facilitated excretion of the metabolites. The low uptake in the intestines (<5%IA/g) and content at 4 h p.i. (Tables 2 and 3) found in the present study shows that Affibody molecules extended by a chelator sequence containing two glutamic acids and one serine still retain a low level of hepatobiliary excretion.

In agreement with previous data using ^{111}In and ^{99m}Tc labelled Affibody molecules [16, 23], modification of the chelator sequence did not have a negative effect on the HER2-binding properties of the Affibody molecules. All different $Z_{HER2:342}$ conjugates have subnanomolar binding affinity to HER2 and high tumour uptake (the average tumour-to-blood ratio at 4 h p.i. was higher than 50 for all three new constructs, see Table 2). The low level of abdominal radioactivity did not interfere with the high contrast imaging of xenografts (Fig. 4). The low uptake values in stomach and salivary gland indicate that there was no release of free pertechnetate into blood circulation during renal catabolism of these conjugates.

Substitution of one glutamic acid residue in the maEEE chelator by serine caused a significant ($p<0.005$) reduction of the renal uptake at 4 h p.i. for ^{99m}Tc-maESE-$Z_{HER2:342}$ to one third compared with ^{99m}Tc-maEEE-$Z_{HER2:342}$. Moreover, the renal uptake of ^{99m}Tc-maESE-$Z_{HER2:342}$ was significantly ($p<0.001$) lower than the uptake of the two other variants. Analysis of urine demonstrated that ^{99m}Tc was present as small radiocatabolites, while the amount of intact ^{99m}Tc-maEEE-$Z_{HER2:342}$, ^{99m}Tc-maESE-$Z_{HER2:342}$, ^{99m}Tc-maEES-$Z_{HER2:342}$ and ^{99m}Tc-maSEE-$Z_{HER2:342}$ in

the urine was below the detection limit already 15 min after injection. This is a strong indication that all conjugates were quantitatively reabsorbed in the kidneys. It should be noted that nearly quantitative renal reabsorption has been found earlier for Affibody molecules with residualising ^{111}In labels [13–16]. Therefore, the difference in renal radioactivity accumulation between the tracers in the present study is most likely due to differences in renal retention of radiocatabolites, rather than a difference in the level of reabsorption of labelled tracer. The reduction of the renal radioactivity between 1 and 4 h p.i., which was observed for ^{99m}Tc-maESE-$Z_{HER2:342}$, is also a strong indication that the excretion of renal catabolites is important to obtain a low level of renal radioactivity at later time points. This hypothesis is further supported by the results of the head to head comparison of the most promising tracer, maESE-$Z_{HER2:\ 342}$, with ^{125}I-PIB-$Z_{HER2:342}$ in a paired label study. Significant reduction of tumour uptake because of saturation of binding sites is an evidence of specificity of targeting. To confirm specificity of the tumour uptake, a control group of tumour-bearing animals was pre-injected with a large excess of non-labelled $Z_{HER2:342}$. Both constructs demonstrated specific targeting of HER2-expressing xenografts, the former with superior tumour-to-organ ratio, but the latter with lower renal retention. This suggests that a radioiodinated catabolite (most likely, an iodobenzoic acid–lysine adduct) is excreted more rapidly from renal cells than the catabolites of ^{99m}Tc-maESE-$Z_{HER2:\ 342}$.

In conclusion, a combination of two glutamic acids and one serine in a mercaptoacetyl-containing chelator allows for a stable labelling of Affibody molecules with ^{99m}Tc. Synthetic Affibody molecules, which are labelled using these chelators, are cleared predominantly via the kidneys with low accumulation of radioactivity in intestinal tract. At the same time, the renal retention of radioactivity was lower in comparison with mercaptoacetyl-triglutamyl-labelled Affibody molecules. The most pronounced reduction of renal uptake was observed in the case of ^{99m}Tc-maESE-$Z_{HER2:342}$. This conjugate provided specific and high contrast imaging of HER2-expressing xenografts at the day of injection.

Acknowledgement Financial support was provided by the Swedish Cancer Society (Cancerfonden) and the Swedish Research Council (Vetenskapsrådet).

References

1. Britz-Cunningham SH, Adelstein SJ. Molecular targeting with radionuclides: state of the science. J Nucl Med 2003;44:1945–61.
2. Boswell CA, Brechbiel MW. Development of radioimmunotherapeutic and diagnostic antibodies: an inside-out view. Nucl Med Biol 2007;34:757–78.
3. Behr TM, Gotthardt M, Barth A, Behe M. Imaging tumors with peptide-based radioligands. Q J Nucl Med 2001;45:189–200.
4. Batra SK, Jain M, Wittel UA, Chauhan SC, Colcher D. Pharmacokinetics and biodistribution of genetically engineered antibodies. Curr Opin Biotechnol 2002;13:603–8.
5. Huhalov A, Chester KA. Engineered single chain antibody fragments for radioimmunotherapy. Q J Nucl Med Mol Imaging 2004;48:279–88.
6. Cortez-Retamozo V, Lauwereys M, Hassanzadeh Gh G, Gobert M, Conrath K, Muyldermans S, et al. Efficient tumor targeting by single-domain antibody fragments of camels. Int J Cancer 2002;98:456–62.
7. Binz HK, Amstutz P, Pluckthun A. Engineering novel binding proteins from nonimmunoglobulin domains. Nat Biotechnol 2005;23:1257–68.
8. Tolmachev V, Orlova A, Nilsson FY, Feldwisch J, Wennborg A, Abrahmsen L. Affibody molecules: potential for in vivo imaging of molecular targets for cancer therapy. Expert Opin Biol Ther 2007;7:555–68.
9. Nilsson FY, Tolmachev V. Affibody molecules: new protein domains for molecular imaging and targeted tumor therapy. Curr Opin Drug Discov Devel 2007;10:167–75.
10. Orlova A, Magnusson M, Eriksson TL, Nilsson M, Larsson B, Hoiden-Guthenberg I, et al. Tumor imaging using a picomolar affinity HER2 binding affibody molecule. Cancer Res 2006;66:4339–48.
11. Hudis CA. Trastuzumab–mechanism of action and use in clinical practice. N Engl J Med 2007;357:39–51.
12. Zidan J, Dashkovsky I, Stayerman C, Basher W, Cozacov C, Hadary A. Comparison of HER-2 overexpression in primary breast cancer and metastatic sites and its effect on biological targeting therapy of metastatic disease. Br J Cancer 2005;93: 552–6.
13. Tolmachev V, Nilsson FY, Widstrom C, Andersson K, Rosik D, Gedda L, et al. ^{111}In-benzyl-DTPA-$Z_{HER2:342}$, an affibody-based conjugate for in vivo imaging of HER2 expression in malignant tumors. J Nucl Med 2006;47:846–53.
14. Orlova A, Tolmachev V, Pehrson R, Lindborg M, Tran T, Sandstrom M, et al. Synthetic affibody molecules: a novel class of affinity ligands for molecular imaging of HER2-expressing malignant tumors. Cancer Res 2007;67:2178–86.
15. Orlova A, Rosik D, Sandstrom M, Lundqvist H, Einarsson L, Tolmachev V. Evaluation of [$^{111/114m}$In]CHX-A″-DTPA-$Z_{HER2:342}$, an Affibody ligand conjugate for targeting of HER2-expressing malignant tumors. Q J Nucl Med Mol Imaging 2007;51:314–23.
16. Orlova A, Tran T, Widstrom C, Engfeldt T, Eriksson Karlstrom A, Tolmachev V. Pre-clinical evaluation of [^{111}In]-benzyl-DOTA-$Z_{HER2:342}$, a potential agent for imaging of HER2 expression in malignant tumors. Int J Mol Med 2007;20:397–404.
17. Baum R, Orlova A, Tolmachev V, Feldwisch J. Receptor PET/CT and SPECT using an Affibody molecule for targeting and molecular imaging of HER2 positive cancer in animal xenografts and human breast cancer patients. J Nucl Med (Supplement 1) 2006;47:108P.
18. Feldwisch J, Orlova A, Tolmachev V, Baum R. Clinical and preclinical application of HER2-specific Affibody molecules for diagnosis of recurrent HER2 positive breast cancer by SPECT or PET/CT. Mol Imaging 2006;5:215.
19. Friedman M, Nordberg E, Hoiden-Guthenberg I, Brismar H, Adams GP, Nilsson FY, et al. Phage display selection of Affibody molecules with specific binding to the extracellular domain of the epidermal growth factor receptor. Protein Eng Des Sel 2007; 20:189–99.
20. Nordberg E, Friedman M, Gostring L, Adams GP, Brismar H, Nilsson FY, et al. Cellular studies of binding, internalization and retention of a radiolabeled EGFR-binding affibody molecule. Nucl Med Biol 2007;34:609–18.

21. Engfeldt T, Orlova A, Tran T, Bruskin A, Widstrom C, Karlstrom AE, et al. Imaging of HER2-expressing tumours using a synthetic Affibody molecule containing the ^{99m}Tc-chelating mercaptoacetyl-glycyl-glycyl-glycyl (MAG3) sequence. Eur J Nucl Med Mol Imaging 2007;34:722–33.
22. Engfeldt T, Tran T, Orlova A, Widstrom C, Feldwisch J, Abrahmsen L, et al. ^{99m}Tc-chelator engineering to improve tumour targeting properties of a HER2-specific Affibody molecule. Eur J Nucl Med Mol Imaging 2007;34:1843–53.
23. Tran T, Engfeldt T, Orlova A, Sandstrom M, Feldwisch J, Abrahmsen L, et al. ^{99m}Tc-maESE-$Z_{HER2:342}$, an Affibody molecule-based tracer for the detection of HER2 expression in malignant tumors. Bioconjug Chem 2007;18:1956–64.
24. Engfeldt T, Renberg B, Brumer H, Nygren PA Karlstrom AE. Chemical synthesis of triple-labelled three-helix bundle binding proteins for specific fluorescent detection of unlabelled protein. Chembiochem 2005;6:1043–50.
25. Tran T, Engfeldt T, Orlova A, Widstrom C, Bruskin A, Tolmachev V, et al. In vivo evaluation of cysteine-based chelators for attachment of ^{99m}Tc to tumor-targeting Affibody molecules. Bioconjug Chem 2007;18:549–58.
26. Behr TM, Goldenberg DM, Becker W. Reducing the renal uptake of radiolabeled antibody fragments and peptides for diagnosis and therapy: present status, future prospects and limitations. Eur J Nucl Med 1998;25:201–12.
27. Melis M, Krenning EP, Bernard BF, Barone R, Visser TJ, de Jong M. Localisation and mechanism of renal retention of radiolabelled somatostatin analogues. Eur J Nucl Med Mol Imaging 2005; 32:1136–43.
28. de Jong M, Barone R, Krenning E, Bernard B, Melis M, Visser T, et al. Megalin is essential for renal proximal tubule reabsorption of ^{111}In-DTPA-octreotide. J Nucl Med 2005;46:1696–700.
29. Rolleman EJ, Valkema R, de Jong M, Kooij PP, Krenning EP. Safe and effective inhibition of renal uptake of radiolabelled octreotide by a combination of lysine and arginine. Eur J Nucl Med Mol Imaging 2003;30:9–15.
30. Behe M, Kluge G, Becker W, Gotthardt M, Behr TM. Use of polyglutamic acids to reduce uptake of radiometal-labeled minigastrin in the kidneys. J Nucl Med 2005;46:1012–5.
31. Vegt E, Wetzels JF, Russel FG, Masereeuw R, Boerman OC, van Eerd JE, et al. Renal uptake of radiolabeled octreotide in human subjects is efficiently inhibited by succinylated gelatin. J Nucl Med 2006;47:432–6.
32. Gotthardt M, van Eerd-Vismale J, Oyen WJ, de Jong M, Zhang H, Rolleman E, et al. Indication for different mechanisms of kidney uptake of radiolabeled peptides. J Nucl Med 2007;48:596–601.
33. Bushnell D, Menda Y, O'Dorisio T, Madsen M, Miller S, Carlisle T, et al. Effects of intravenous amino acid administration with Y-90 DOTA-Phe1-Tyr3-Octreotide (SMT487[OctreoTher) treatment. Cancer Biother Radiopharm 2004;19:35–41.